LAWRENCE
LIVERMORE
NATIONAL
LABORATORY

LLNL-JRNL-674877

Improved Precision and Accuracy in Quantifying Plutonium Isotope Ratios by RIMS

B. H. Isselhardt, M. R. Savina, A. Kucher, S. D. Gates, K. B. Knight, I. D. Hutcheon

July 20, 2015

Journal of Radioanalytical and Nuclear Chemistry

Disclaimer

Title page

Special Issue (SI): MARC X

Log number of paper: 553

Names of the authors: B.H. Isselhardt[1], M.R. Savina[1,2], A. Kucher[1], S.D. Gates[1], K.B. Knight[1], I.D. Hutcheon[1]

Title: Improved Precision and Accuracy in Quantifying Plutonium Isotope Ratios by RIMS

Affiliation(s) and address(es) of the author(s): (1) LLNL, (2) ANL

1 Lawrence Livermore National Laboratory, PO Box 808, L-231, Livermore, CA 94551 USA

2 Argonne National Laboratory, 9700 South Cass Ave., Argonne, IL 60439 USA

E-mail address of the corresponding author: isselhardt1@llnl.gov, (925)-424-3347

Improved Precision and Accuracy in Quantifying Plutonium Isotope Ratios by RIMS

B.H. Isselhardt[1], M.R. Savina[2†], A. Kucher[1], S.D. Gates[1], K.B. Knight[1], I.D. Hutcheon[1]

[1]*Lawrence Livermore National Laboratory, 7000 East Ave., Livermore, CA 94551 USA*

[2]*Argonne National Laboratory, 9700 South Cass Ave., Argonne, IL 60439 USA*

[†]*Present affiliation: Lawrence Livermore National Laboratory*

Abstract

Resonance ionization mass spectrometry (RIMS) holds the promise of rapid, isobar-free quantification of actinide isotope ratios in as-received materials (i.e. not chemically purified). Recent progress in achieving this potential using two Pu test materials is presented. RIMS measurements were conducted multiple times over a period of two months on two different Pu solutions deposited on metal surfaces. Measurements were bracketed with a Pu isotopic standard, and yielded absolute accuracies of the measured $^{240}Pu/^{239}Pu$ ratios of 0.7% and 0.58%, with precisions (95% confidence intervals) of 1.49% and 0.91%. The minor isotope ^{238}Pu was also quantified despite the presence of a significant quantity of ^{238}U in the samples.

Keywords

resonance ionization mass spectrometry, nuclear forensics, plutonium, isotope ratios, laser post-ionization

Introduction

Current techniques for determining U and Pu isotopic compositions in solid samples for nuclear forensics, safeguards, and security applications often require lengthy analysis times. This is largely the result of the sample preparation techniques required to remove isobaric interferences prior to analysis by mass-based analytical techniques, which may take several days to complete[1]. New techniques such as capillary electrophoresis inductively coupled plasma mass spectrometry (CE-ICP-MS)[2] and high performance liquid chromatography inductively coupled plasma mass spectrometry (HPLC-ICP-MS)[3] have recently shown potential in reducing analysis times. However, these methods still require chemical dissolution, and the multiple valence states of actinide elements can create additional challenges. Secondary ion mass spectrometry (SIMS) is effective in analyzing solid samples with minimal preparation, and has recently demonstrated excellent precision and sensitivity on uranium oxide reference materials[4,5]. However, SIMS can be affected by the presence of isobaric interferences from same-mass isotopes of other elements, hydrides and other molecular compounds (e.g., $^{27}Al^{208}Pb$, m/z = 235; see ref. [4] for an exhaustive list of uranium molecular isobars). While elemental isobaric interference in the actinide mass range (e.g., $^{238}U/^{238}Pu$) cannot be resolved by SIMS, large geometry magnetic sector instruments can in principle resolve most molecular isobaric interferences, except for hydrides[4].

Resonance ionization mass spectrometry (RIMS) is suited to address the challenges posed by isobaric interference in isotopic analyses. In brief, a solid sample of the material is placed in the instrument and a pulsed laser or ion beam incident on the sample generates an expanding cloud of ions and neutral atoms and molecules above the sample. The secondary ions generated during this process are electrostatically rejected by applying a pulsed voltage to the sample, leaving the neutral species behind. Neutral atoms of the element of interest are then resonantly excited to an intermediate electronic state by the absorption of one or more laser photons. This resonant excitation can be accomplished via a single excitation or can be made more selective through the use of two or more resonant steps. The excited atoms are then photoionized from the intermediate electronic state by an additional laser, generally tuned to either an autoionizing resonance (an unbound metastable state) above the ionization potential, or a

high-lying Rydberg state that is ionized by the electric field of the ion extraction optics. Finally, these photoions are accelerated into a mass spectrometer and detected [6].

Similar to SIMS, RIMS does not require sample pretreatment. Isobaric interferences are avoided since other elements are generally transparent at wavelengths specific to the analyte of interest. Moreover, as resonance ionization processes are often saturated, RIMS has the potential to achieve very high useful yield for most elements (defined as the number of atoms detected per atom consumed during analysis). Improvements in useful yield can serve to increase analytical precision and/or reduce analytical time lines.

The reproducibility of isotope ratio measurements by RIMS is very sensitive to the wavelength stability of the resonance laser. Resonance ionization can produce large isotopic fractionation primarily due to two causes: 1) isotope shifts, in which the isotopes of a single element all have different electronic excitation energies, and 2) odd-even isotope effects, in which hyperfine splitting in odd isotopes leads to unequal photoionization rates [7,8]. Heavy elements such as actinides have large isotope shifts. Plutonium is a challenging element to analyze for isotopic composition in part because at resonances useful for RIMS it has isotope shifts as large as 20 pm between ^{238}Pu and ^{242}Pu. Isselhardt, *et al.* demonstrated that fluctuations in the laser wavelength of that magnitude can cause the measured ^{235}U/^{238}U ratio of uranium, which has a smaller isotope shift of 7pm, to change by over two orders of magnitude [9].

Key parameters affecting the precision of isotopic measurements by RIMS include the ratio of the laser bandwidth to the isotope shift, as well as the degree of laser power broadening of the electronic transitions (the increase in the apparent width of an atomic absorption line due to laser intensity) [10,11]. Reproducibility is also affected by fluctuations in laser parameters such as power, bandwidth, and the timing and temporal width of laser pulses during the measurement. While the precision of RIMS isotope ratio measurements has been reported for a number of elements including plutonium, no systematic assessments of the sources of ion backgrounds and the ultimate achievable precision and accuracy have been undertaken. Published RIMS measurements have demonstrated precision in the ^{240}Pu/^{239}Pu ratio ranging from 0.24% [12] to several

percent [13-15]. These studies reported uncorrected isotope ratios (i.e. the ratios were not normalized to a standard), and did not explicitly demonstrate the reproducibility of Pu isotope ratio quantification by RIMS over multiple measurement campaigns or to accuracies better than several percent.

The RIMS studies cited above have used fundamentally different spectroscopic approaches. Donohue [12] used pulsed lasers at relatively high power to ionize thermally evaporated neutral Pu atoms. The combination of Doppler and power broadening, together with the relatively wide spectral bandwidth of the pulsed lasers, allowed all isotopes to be ionized simultaneously, albeit at varying efficiencies. In contrast, Gruning *et al.* [13] (reviewed in Trautmann *et al.* [15]), and Raeder *et al.* [14] used pulsed Ti:Sapphire lasers with relatively narrow (~3 GHz) bandwidth. To avoid spectroscopic fractionation, these authors tuned the lasers to individual isotopes in sequence.

Our spectroscopic approach is similar to the former study, *i.e.* simultaneous ionization of all isotopes. In contrast to the Donahue study, which used a low repetition rate (30 Hz) dye laser with 90 GHz bandwidth, our Ti:Sapphire lasers had bandwidths from 5 to 25 GHz, depending on the wavelength (shorter wavelengths had higher bandwidths). Our laser pulse energy was also an order of magnitude lower, and so likely resulted in less power broadening of the transitions. However, the Donahue *et al.* study used a single laser tuned to a single Pu resonance, resulting in a one-color, three-photon ionization scheme. The first step was resonant and the second step was quasi-resonant (i.e. at the edge of the laser bandwidth), while the third step was non-resonant. The mismatch between the laser and transition energies would be expected to reduce the power broadening significantly. Isotopic fractionation was indeed observed, at the level of 2% for the $^{240}Pu/^{239}Pu$ ratio, against an internal precision of 0.25%. To account for fractionation in a method that relies on simultaneous ionization of all isotopes, we used standard/sample bracketing. This accounts for all sources of fractionation, including spectroscopic.

The present study focused on the development of RIMS for rapid isotopic analysis of plutonium using a 3-color, 3-photon resonance ionization scheme and standard/sample bracketing. We present RIMS isotopic measurements on plutonium with attention to the

characterization of backgrounds and competing ionization processes. We use these measurements to demonstrate a rapid, robust method for routine *in situ* measurement of plutonium isotopes in solid materials, using Pu electrodeposited onto Ti and Ta surfaces as samples.

Method

Samples and Sample Preparation

In order to determine the current accuracy and precision of measured Pu isotope ratios achievable by RIMS using the CHARISMA instrument at Argonne National Laboratory, three samples with well-characterized Pu isotopic abundances were selected. The first sample CRM137 was chosen for use as a standard to correct measured isotope ratios for instrumental fractionation. Two additional samples, Sample A and Sample B, were also selected to serve as "unknown" samples, due to their well-characterized Pu isotope abundances which would allow for better assessment of measurement performance. The Pu isotope ratios of all three samples are given in Table 1. The values for CRM137 are age-corrected declared values (determined by TIMS, New Brunswick Laboratory), while those of the two "unknown" samples were measured by MC-ICP-MS at Lawrence Livermore National Laboratory after purification by column chromatography. Due to the presence of ^{238}U even in the purified samples, the ^{238}Pu/^{239}Pu ratios in Table 1 were not measured directly by MC-ICP-MS. The ^{238}Pu/$^{239+240}$Pu ratio was measured by alpha spectrometry, and the ^{240}Pu/^{239}Pu ratio determined by MC-ICP-MS was used to convert that ratio to ^{238}Pu/^{239}Pu. All three materials were available as dilute solutions in 2% nitric acid, with Pu concentrations of about 10 μg/mL. None of the sample solutions were chemically purified prior to RIMS sample preparation; all of the samples contained unknown amounts of U, Np, and Am from incomplete chemical separation during production and from the decay of Pu. The use of as-received solutions without purification was intended to evaluate the insensitivity of RIMS to the presence of isobaric interferences. The use of sample electrodeposited on metal surfaces was intended to evaluate the claim that RIMS is useful for the *in situ* analysis of solid materials.

Table 1: Known isotope ratios of samples used in this study, at 95% confidence. See text for analysis methods.

Sample	$^{238}Pu/^{239}Pu$	$^{240}Pu/^{239}Pu$	$^{241}Pu/^{239}Pu$	$^{242}Pu/^{239}Pu$
CRM137	0.00280(6)	0.2408(3)	0.00755(2)	0.01561(5)
Sample A	0.00287(3)	0.2410(4)	0.00760(6)	0.0156(1)
Sample B	0.000118(3)	0.0625(1)	0.000848(8)	0.000398(5)

The sample solutions were prepared for analysis by electrodeposition in fresh custom cells, shown in Fig. 1, constructed with an aluminum base and Delrin body, with the bottom of the cell machined to match the dimensions of the sample stub. The samples were deposited onto 8 mm diameter Ti or Ta metal stubs, with pins for holding them into our multi-sample holder (see Fig. 2). The faces of the stubs were lightly polished to remove machining defects and provide a smooth surface for deposition. A central 2 mm diameter, 25 mm long hole in the cell defined the sample spot, producing a cell volume of 0.5 ml. Aliquots of 10^{11} to 10^{12} atoms of the sample were dissolved in 30 µl of 0.05 M HNO_3 and introduced into the cell along with 200 µl of isopropanol. A platinum wire with a small loop bent into one end was used to stir the solution, then fixed in the cell a few mm above the top of the sample stub. A 300 W power supply was attached to the Pt wire and the Al base plate. The current limit was set to 4 mA, and the maximum potential noted during the approximately 3 hour elecrodeposition was 315 V. After depsosition the cell was drained with a glass Pasteur pipet, and the sample stub was removed and allowed to dry. In practice the deposited spots were ~3 mm in diameter (Fig. 2), resulting in an average Pu surface coverage of ~10^{-3} to 10^{-2} monolayers. Duplicate stubs were produced for each of the samples to investigate intra-sample variation in the CHARISMA instrument. Samples were mounted for analysis in groups of four in 75 mm aluminum targets to enable switching between samples.

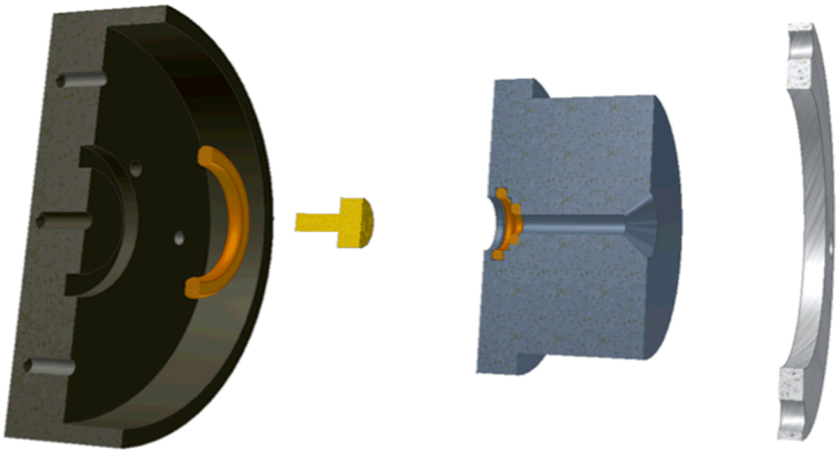

Fig. 1 Exploded cross-section view of the electro-deposition cell used to prepare samples.

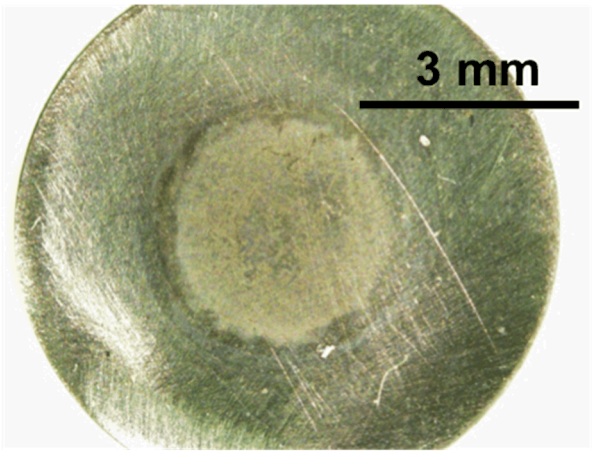

Fig. 2 Optical micrograph of Sample B electrodeposited onto a Ti stub into a ~3 mm diameter spot. Total deposited sample mass was ~15 ng of Pu.

Resonance Ionization Mass Spectrometry

RIMS measurements were done on the CHARISMA instrument at Argonne National Laboratory, described in detail elsewhere [6]. The analytical setup was similar to that described by Isselhardt *et al*. [8]. Briefly, the samples were probed using the third-harmonic output of a Nd:YLF laser at 351 nm, with a pulse duration of 25 ns, focused to a ~500 μm diameter spot. The secondary ions produced by laser desorption were ejected with a 4 kV pulse of 1200 ns duration, such that their background contributions were vanishingly small. Two hundred nanoseconds after the end of the ion ejection pulse, the

187 laser-desorbed neutrals were resonantly ionized with pulsed laser beams passing ~1 mm
188 above and parallel to the sample surface. Two hundred nanoseconds after the laser pulse,
189 the generated photoions were accelerated by a 2 kV extraction pulse into a reflectron
190 time-of-flight mass spectrometer.

191 Ions were detected by a microchannel plate detector and recorded by a time-to-digital
192 converter. Count rates were generally kept low (< 0.03 ions per laser pulse in a single 200
193 ps time bin) to avoid large dead time corrections [16]. The repetition rate of the system
194 was 1.4 kHz. The results of fifty thousand laser shots were summed to produce a single
195 mass spectrum, and anywhere from 20 to 110 spectra were summed to reduce statistical
196 uncertainty in the measured isotope ratios.

197 *Description of lasers and the ionization scheme*

198 Resonance and ionization lasers were grating-tuned Ti:Sapphire systems essentially
199 identical to those previously described [10,6]. Wavelengths shorter than the 700 - 1000
200 nm tuning range of the lasers were generated by intra-cavity frequency doubling using
201 lithium triborate crystals. The laser bandwidth was adjustable in steps by using various
202 combinations of anamorphic prism pairs with expansion ratios ranging from X2 to X28,
203 in order to set the number of illuminated lines on the intra-cavity grating. The bandwidths
204 of the lasers ranged from 10 to 20 pm. An automated feedback control system was used
205 to correct for long-term wavelength drift [10]. Temporal pulse widths were 15 to 20 ns.
206 The beams were focused to FWHM diameters between 1 and 1.3 mm each and passed in
207 a collinear geometry ~1 mm above and parallel to the sample surface, such that ~5% of
208 the laser power was occluded by the sample mount.

209 Our 3-color ionization scheme was based on the work of Gruning *et al.* [13], who
210 determined the Pu isotope shifts for a set of resonances easily accessible by Ti:Sappire
211 lasers. In our measurement the two resonance transitions were well saturated, whereas the
212 ionizing transition was close to saturation. We chose to utilize an ionizing laser
213 wavelength of 767.530 nm (Fig. 3), corresponding to a total energy of 48,597.65 cm^{-1},
214 which is between two Rydberg states reported by Gruning *et al*. The two resonance lasers
215 were tuned to the midpoints between the ^{239}Pu and ^{240}Pu transition wavelengths. An

autoionizing resonance reported in the literature [14] was also tested for the final transition at 750.24 nm, however we observed an ion yield for this transition of about a factor of two lower than for the Rydberg state.

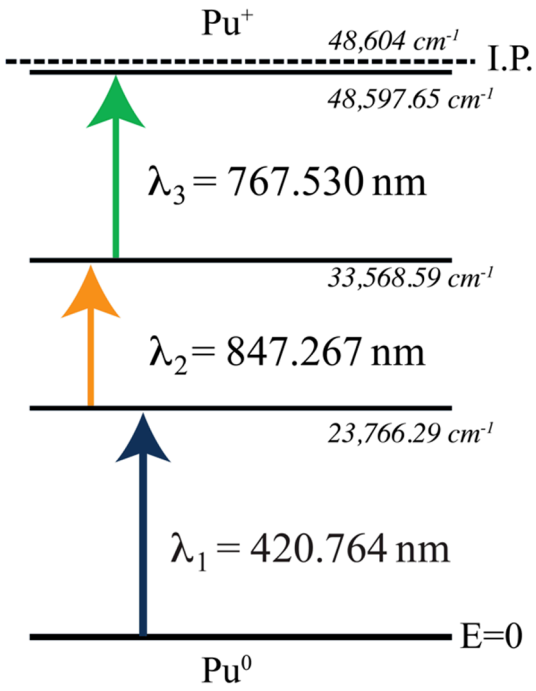

Fig. 3 Pu ionization scheme employed in this study, showing the energies of the levels used and the laser wavelengths used to excite each transition.

Results and discussion

Resonance and background ion signals in the Pu mass region

When analyzing samples of unknown chemical composition and purity by RIMS it is necessary to separate the analyte of interest from background signals to avoid potential interferences. This is accomplished by comparing the resonance ionization ion yield to the ion yield from off-resonance laser conditions. For off-resonance ionization, the wavelength of one of the lasers, normally the laser involved in the transition between the ground and first excited state, was changed by ~0.5 nm. Changing the wavelength by such a small amount had no effect on the laser power, but reduced the Pu atom photo-

ionization signal by several orders of magnitude. The result was a direct observation of the non-resonant background ion signal. A comparison of the resonant and off-resonance ion signals for test Sample B is shown in Fig. 5, where the first resonance laser was detuned from 420.764 nm to 421.264 nm. The traces represent the average of ten measurements (500,000 acquisition cycles in total) for each ionization condition. Comparing the integrated peaks at *m/z* 239 and 240 for the two conditions yields a ratio for off-resonance ion signal to resonant ion signal of ~0.6%. These measurements were performed for all three samples and the relative off-resonance signals were similar in all cases. The off-resonance peaks have the same Pu isotope distribution as the resonance spectra and likely correspond to photofragmentation of plutonium oxides in the ejecta plume. The exception is the peak at *m/z* 241 in some samples, which is enhanced in the off-resonance spectrum relative to the other Pu peaks. We hypothesize that this is due to the presence of a significant quantity of ^{241}Am, which would be anticipated in an aged and unpurified sample containing ^{241}Pu. Correcting RIMS spectra for off-resonance contributions resulted in insignificant changes to the measured isotope ratios (>>1 σ), therefore off-resonance backgrounds were ignored.

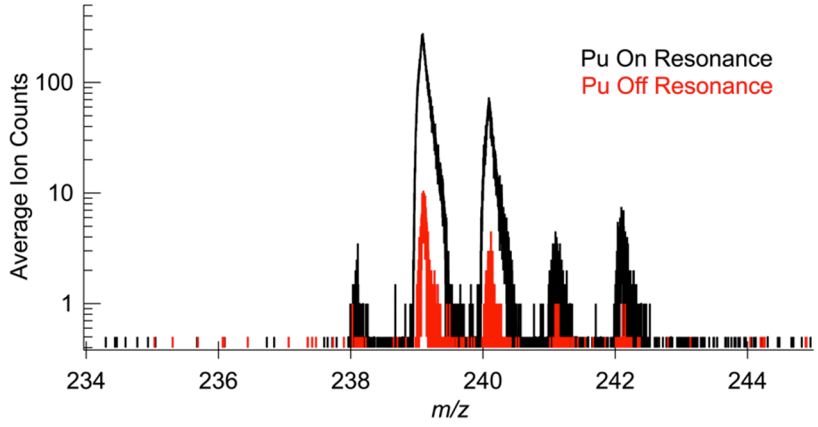

Fig. 5: Resonance ionization spectra from Sample B, with the wavelengths of all three lasers tuned on resonance (black), and the first laser tuned off resonance by 05 nm (red). Each mass spectrum is the average of 10 measurements of 50,000 acquisition cycles each.

Precision and accuracy of Pu isotope ratio measurements

The precision of actinide isotope ratio measurements by RIMS is limited by the stability of laser and ion sources over the periods of time required to make measurements at sufficient precision (see for example ref. [14]). Fig. 6 shows the precision and accuracy of the measured $^{240}Pu/^{239}Pu$ isotope ratio in a sample of CRM137, which we used as the standard to correct for instrument bias in measurements of the two test materials. The data are presented as vertical lines signifying 1σ deviations of the individual measurements (50,000 acquisition cycles each), expressed as the absolute deviation of the measured ratio from the declared value for CRM137. The mean square weighted deviation (MSWD) for the data set was calculated and used to calculate 95% confidence limits. In practice, MSWD was always close to one for all isotope ratio measurements except for some involving ^{241}Pu (see below), and had a neglible effect on calculated uncertainties, indicating that the precision was limited by counting statistics rather than non-statistical uncertainty. The mean of all individual measurements, represented by the dashed line, was -0.74 ± 0.25% (95% confidence interval). Each data point represents 35 seconds of data collection (~32 minutes total). All of the measurements reported below were taken to similar levels of precision in the $^{240}Pu/^{239}Pu$ ratio. Any measurements that did not show similar internal precision were excluded from sample averages. Overall, an instrument-induced measurement bias of less than 1% was measured for this isotope ratio. This is quite small compared to the order-of-magnitude bias that laser-based selective ionization can potentially induce [9].

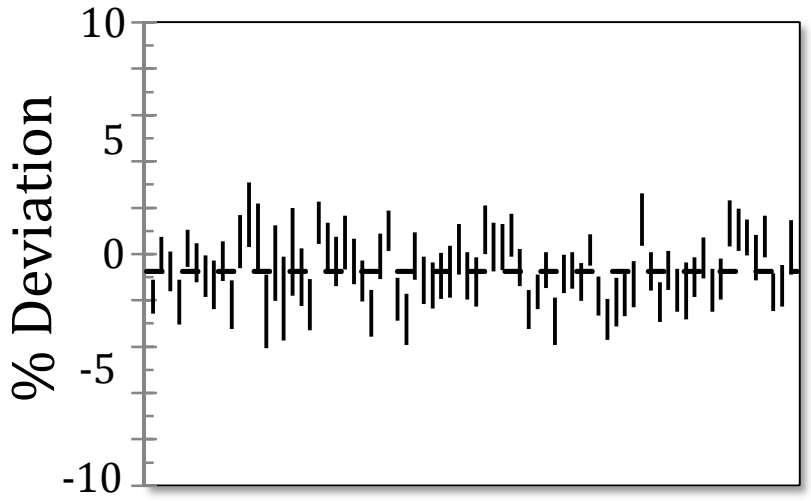

Fig. 6 The absolute deviation of the measured $^{240}Pu/^{239}Pu$ isotope ratio of CRM137 over the course of a run of 55 spectra. Vertical lines represent one standard deviation of each measurement; the dashed line represents the mean of the data set

To obtain accurate quantification of the Pu isotope ratios for the two test samples, we measured CRM137 before and after each pair of test samples to provide for instrument bias correction via standard-sample-standard bracketting. We measured both the standard and the test materials several times over the course of six different days, over a period of about two months. The results from the full sequence of bracketed measurements of the $^{240}Pu/^{239}Pu$ ratio is shown in Fig. 7, and summarized for the other isotope ratios in Table 2. In general the absolute accuracy of individual measurements of $^{240}Pu/^{239}Pu$ was better than 1%, and the 95% confidence intervals for the entire set of measurements were 1.32% for Sample A and 0.71% for Sample B. The minor isotope ratios were also consistent with the stated values within 95% confidence intervals, though the intervals were larger due to low count rates.

Our focus in this study was to determine whether RIMS can acheive high precision and accuracy in as-received (unpurified) samples of Pu. Accordingly, we designed the experiments to be certain of avoiding known artifacts in time-of-flight mass spectrometry. First, ion count rates were kept low to be certain of preventing

undercounting of the abundant isotope due to dead-time effects. This was done by using very low desorbing laser fluence to ensure that the number of neutrals desorbed per pulse was low. While it is possible to correct for dead time effects [16], the error propogation due to the correction degrades the precision of the measurement. Further, rigorous dead time correction is only possible either for desorption events that obey Poisson statistics [16], which is not the case for laser desorption as used in this study, or in cases where correlated ion events can be quantified on a shot-by-shot basis [17]. We chose to rigorously avoid dead time effects and so ran at count rates far below those at which dead time would noticeably affect the data. In addition, to avoid overcounting the abundant isotope due to ringing in the detector line, we set the discrimination level on the MCP output artificially high. This further decreased the count rate by rejecting many legitimate ion counts.

We have shown that our Pu isotope ratio measurement is statistics-limited (i.e. MSWD ~ 1), which means that the precision is set by the number of ion counts observed. In the statistics-limited regime, the precision attained in a fixed measurement time will increase as the square root of the overall count rate. Now that we have demonstrated that good precision and accuracy are routinely attainable with RIMS, we intend to carefully calibrate these two effects (dead time and overcounting) and run future analyses at significantly higher per-pulse count rates. Further, new lasers systems under development will allow the analyses to be done at pulse repetition rates of 2-3 kHz rather than 1.4 kHz, further increasing the overall count rate.

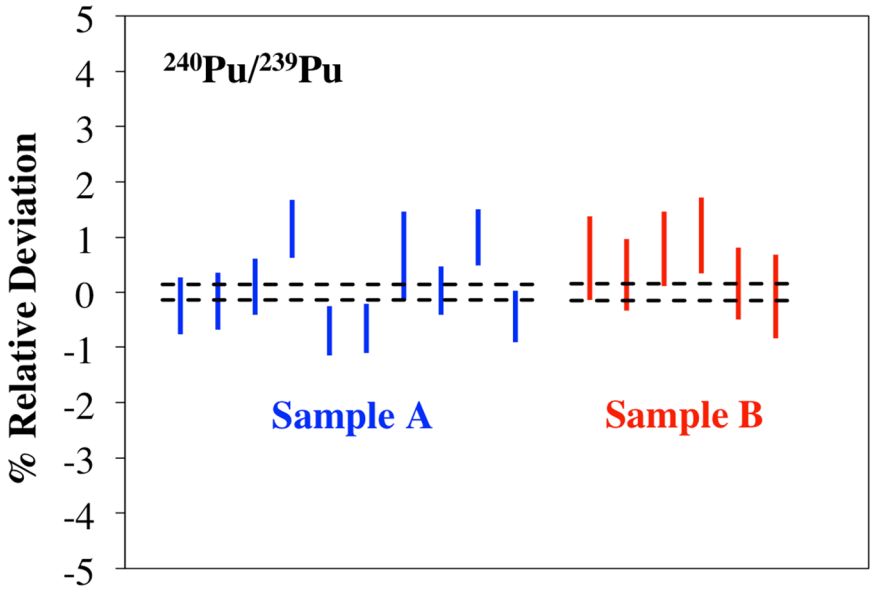

Fig. 7 The $^{240}Pu/^{239}Pu$ ratios measured in the two test materials several times over the course of six different days. Each individual bar corresponds to a single bracketed measurement and represents the 95% confidence interval of that analysis. The dotted lines correspond to the 95% confidence intervals for the MC-ICP-MS measurements.

Table 2 Summary of measured isotope ratios corrected for instrument fractionation using CRM137 and expressed as percent deviation from the 'known' values measured by ICP-MS (see Table 1). The reported mean is the average of the set of measurements for each sample, and the stated uncertainties are 95% confidence intervals that include non-statitistical uncertainties via MSWD. Non-statistical uncertainties were negligible for all ratios except $^{241}Pu/^{239}Pu$.

Ratio	*Sample A (% Deviation)*	*Sample B (% Deviation)*
$^{238}Pu/^{239}Pu$	**-2.36 ± 4.60**	**7.09 ± 22.53**
$^{240}Pu/^{239}Pu$	**0.70 ± 1.49**	**0.58 ± 0.91**
$^{241}Pu/^{239}Pu$	**5.65 ± 38.05**	**21.6 ± 100.1**
$^{242}Pu/^{239}Pu$	**1.37 ± 6.99**	**8.44 ± 13.19**

Isobaric interferences

Because U is a common contaminant in Pu samples we also performed resonance ionization for U isotopes. The resonance ionization scheme for U is given in ref. [9]. Changing the laser wavelengths between the U and Pu schemes required about 15 minutes with our current laser systems. The RIMS spectrum of U in Sample A is shown

in Fig. 8. The figure also includes the off-resonance spectrum for U, where the first resonance laser wavelength of 415.510 nm was changed to 416.010 nm. Comparing the two spectra one can clearly see the U isotopes, with by far the most abundant being ^{238}U. Off-resonance Pu peaks are also observed, and again the ratio of *m/z* 241/240 is much higher than can be explained by the known Pu isotope ratio and is tentatively attributed to ^{241}Am interference. In addition, a small peak at *m/z* 237 likely corresponds to ^{237}Np from ^{241}Am decay.

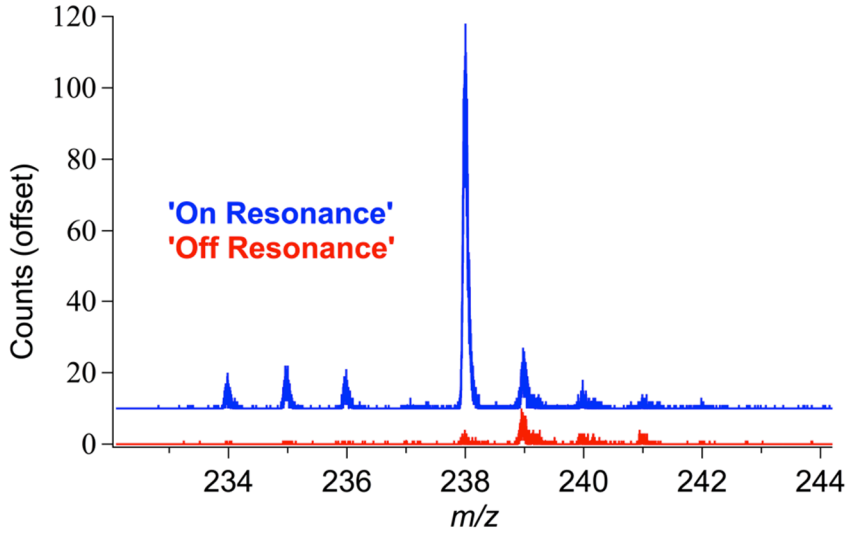

Fig. 8 Comparison of uranium on and off resonance ionization of Sample A

Comparison of the on and off-resonance ion yelds of U and Pu allows an estimation of the relative U and Pu concentrations in the sample. The assumptions are 1) the probability of producing off-resonance Pu ions is equal for both the U off-resonance and Pu off-resonance ionization conditions (an assumption that should be tested in future work), and 2) resonance ionization is largely saturated for both U and Pu. One can then compare the on and off-resonance ion signals for U and Pu to estimate that the Pu/U concentration in this sample is ~50. As alpha spectrometry indicated that approximately 15 ng of Pu was electrodeposited onto this stub, this equates to approximately 0.3 ng of U. More importantly, it yields an estimate for the ^{238}U/^{238}Pu ratio of ~10. Thus, in the absence of prior chemical purification, the RIMS measurement of the ^{238}Pu/^{239}Pu ratio in this sample was performed with the isobaric interferent ^{238}U present in overwhelming abundance. Despite this, Table 2 shows that the ^{238}Pu/^{239}Pu ratio of Sample A was

measured with an absolute accuracy of 2.3%, and was consistent with the MC-ICP-MS / alpha spectrometry measurements within our statistics-limited precision. With appropriate concentration standards and rigorous quantification of the on- and off-resonance ion yields of U and Pu, this approach may yield quantifiable estimates of the relative U and Pu concentrations in unknown samples (or any other pair of elements of interest).

During the course of this investigation it was noted in several samples that the ion signal at *m/z* 241 was highly variable compared to the stability of the other isotope signals and was also very dependent on the lateral position of the measument within a given sample. This is demonstrated in Fig. 9, where a depth profile (ion signal as a fuction of cumulative signal on a given spot) for the *m/z* 241/^{239}Pu ratio is compared to the ^{242}Pu/^{239}Pu ratio during a single analysis of a CRM137 sample. The ^{242}Pu/^{241}Pu ratio is constant within statisical uncertainty over the course of this measurement, but the *m/z* 241/^{239}Pu ratio changes by a factor of 3 during the same period. The stability of the ^{242}Pu/^{239}Pu ratio rules out laser-induced fractionation that would typically be suspected as the cause of the drift, because the ^{242}Pu/^{239}Pu ratio is even more suseptible to laser drift than is the ^{241}Pu/^{239}Pu ratio. An investigation of the off-resonance ionization ion signal at *m/z* 241 in this sample showed a significant dependence on wavelength that is highly atypical of non-resonant ionization signals. We hypothesize that the large variability in the ion signal at *m/z* 241 is due to a resonance-enhanced multiphoton ionization (REMPI) process driving the dissociation of an Am molecular species present in the neutral ejecta from this sample, coupled with an inhomogeneous distribution of the molecular species in our electro-deposited samples. Experiments to study this observation and minimize its effect on the ability to quantify ^{241}Pu in these samples are currently being planned. Without the precision and accuracy currently being demonstrated by RIMS, these effects would be nearly impossible to isolate and diagnose.

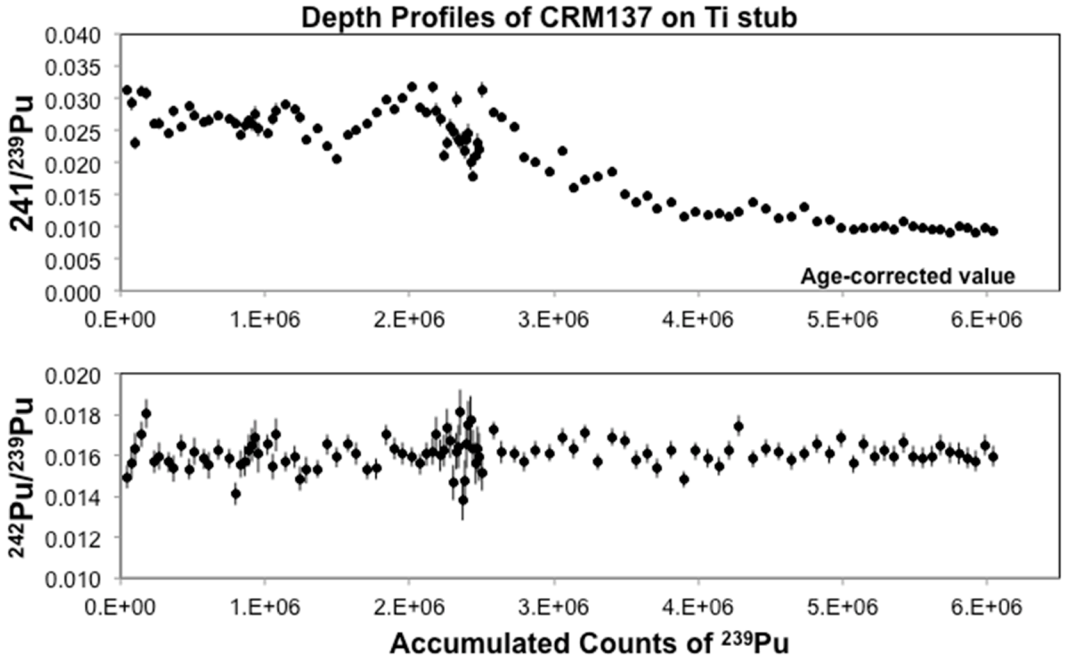

Fig. 9 Depth profiles of CRM137 for both *m/z* 241/^{239}Pu and ^{242}Pu/^{239}Pu during the analysis of a single sample. The ion signal at *m/z* 241 is highly variable. The stability of the other measured isotope ratios eliminate laser induced fractionation as the source of this variation.

Conclusions

We report the quantification of Pu isotope ratios by RIMS to high precision and accuracy, on the order of 1%. These measurements represent the developing capabilities of RIMS at LLNL/ANL to quantify actinide isotope ratios. Statistics-limited precisions in the reported minor isotope ratios ^{238}Pu/^{239}Pu, ^{241}Pu/^{239}Pu, and ^{242}Pu/^{239}Pu were demonstrated, although presumed ^{241}Am based interference led to large uncertainties in the measured ^{241}Pu/^{239}Pu ratios in some samples. This interference is the subject of ongoing studies to determine its wavelength dependence, in order to better identify it and refine the Pu ionization scheme to avoid it in future analyses.

Acknowledgements

The authors dedicate this work to the memory and inspiration of our mentor Dr. Ian D. Hutcheon, without whom this work would not have been possible. The authors would also like to thank Dr. Roger Henderson, Dr. Ross Williams, Dr. Amy Gaffney for their help in sample preparation and sample characterization. This work was funded by the U.S. Department of Homeland Security National Technical Nuclear Forensics Center and Laboratory Directed Research and Development Program at LLNL under project 14-ER-082. This work performed under the auspices of the U.S. Department of Energy by Lawrence Livermore National Laboratory under Contract DE-AC52-07NA27344. The CHARISMA instrument at Argonne is supported by the U.S. Department of Energy,

Basic Energy Sciences, Division of Material Sciences and Engineering under Award No. DE-AC02-06CH11357. LLNL-JRNL-PENDING.

References

1. Hou X, Roos P (2008) Critical comparison of radiometric and mass spectrometric methods for the determination of radionuclides in environmental, biological and nuclear waste samples. Analytica Chimica Acta 608:105-139

2. Pitois A, Heras LAdL, Betti M (2008) Determination of fission products in nuclear samples by capillary electrophoresis-inductively coupled plasma mass spectrometry (CE-ICP-MS). International Journal of Mass Spectrometry 270 (3):118-126. doi:10.1016/j.ijms.2007.11.012

3. Günther-Leopold I, Waldis JK, Wernli B, Kopajtic Z (2005) Measurement of plutonium isotope ratios in nuclear fuel samples by HPLC-MC-ICP-MS. International Journal of Mass Spectrometry 242 (2-3):197-202. doi:10.1016/j.ijms.2004.11.007

4. Ranebo Y, Hedberg PML, Whitehouse MJ, Ingeneri K, Littmann S (2009) Improved isotopic SIMS measurements of uranium particles for nuclear safeguard purposes. Journal of Analytical Atomic Spectrometry 24 (3):277-287. doi:10.1039/b810474c

5. Ranebo Y, Niagolova N, Erdmann N, Eriksson M, Tamborini G, Betti M (2010) Production and Characterization of Monodisperse Plutonium, Uranium, and Mixed Uranium-Plutonium Particles for Nuclear Safeguard Applications. Analytical Chemistry 82 (10):4055-4062. doi:10.1021/ac9029295

6. Savina MR, Pellin MJ, Tripa CE, Veryovkin IV, Calaway WF, Davis AM (2003) Analyzing individual presolar grains with CHARISMA. Geochim Cosmochim Acta 67 (17):3215-3225

7. Wunderlich RK, Hutcheon ID, Wasserburg GJ, Blake GA (1992) Laser-induced isotopic selectivity in the resonance ionization of osmium. Int J Mass Spectrom Ion Processes 115 (2-3):123-155

8. Wunderlich RK, Wasserburg GJ, Hutcheon ID, Blake GA (1993) Laser-induced isotopic effects in titanium resonance ionization. Anal Chem 65 (10):1411-1418

9. Isselhardt BH, Savina MR, Knight KB, Pellin MJ, Hutcheon ID, Prussin SG (2011) Improving Precision in RIMS: The Influence of Bandwidth in Uranium Isotope Ratio Measurements. Analytical Chemistry 83:2469-2475. doi:dx.doi.org/10.1021/ac102586v

10. Levine J, Savina M, Stephan T, Dauphas N, Davis AM, Knight K, Pellin M (2009) Resonance ionization mass spectrometry for precise measurements of isotope ratios. International Journal of Mass Spectrometry 288:36-43

11. Levine J, Savina M, Stephan T, Pellin M Improvements in RIMS Isotopic Precision: Applications to in situ atom-limited isotopic analyses In: Iguchi T, Watanabe K (eds) 4th

International Conference on Laser Probing, Nagoya, Japan, 2009. American Institute of Physics, pp 90-95

12. Donohue DL, Smith DH, Young JP, McKown HS, Pritchard CA (1984) Isotopic analysis of uranium and plutonium mixtures by resonance ionization mass spectrometry. Anal Chem 56 (3):379-381

13. Gruning C, Huber G, Klopp P, Kratz JV, Kunz P, Passler G, Trautmann N, Waldek A, Wendt K (2004) Resonance ionization mass spectrometry for ultratrace analysis of plutonium with a new solid state laser system. International Journal of Mass Spectrometry 235 (2):171

14. Raeder S, Hakimi A, Stöbener N, Trautmann N, Wendt K (2012) Detection of plutonium isotopes at lowest quantities using in-source resonance ionization mass spectrometry. Analytical and Bioanalytical Chemistry 404 (8):2163-2172. doi:10.1007/s00216-012-6238-6

15. Trautmann N, Passler G, Wendt KDA (2004) Ultratrace analysis and isotope ratio measurements of long-lived radioisotopes by resonance ionization mass spectrometry (RIMS). Analytical and Bioanalytical Chemistry 378 (2):348-355. doi:10.1007/s00216-003-2183-8

16. Stephan T, Zehnpfenning J, Benninghoven A (1994) Correction of dead time effects in time-of-flight mass spectrometry. Journal of Vacuum Science & Technology A: Vacuum, Surfaces, and Films 12 (2):405-410

17. Stephan T, Heck PR, Isheim D, Lewis JB (2015) Correction of dead time effects in laser-induced desorption time-of-flight mass spectrometry: Applications in atom probe tomography. International Journal of Mass Spectrometry 379 (0):46-51. doi:http://dx.doi.org/10.1016/j.ijms.2014.12.006